Reservoir Porosity Measurement Uncertainty and its Influence on Shale Gas Resource Assessment

TIAN Hua [1,2,3,*], ZOU Caineng [1], LIU Shaobo [1,3], HONG Feng [1,3], FAN Junjia [1,3], Gui Lili [1,3] and HAO Jiaqing [1,3]

[1] *Research Institute of Petroleum Exploration and Development, PetroChina, Beijing 100083, China*

[2] *Key Laboratory of Petroleum Geochemistry, CNPC, Beijing 100083, China*

[3] *Key Laboratory of Basin Structure and Hydrocarbon Accumulation, CNPC, Beijing 100083, China*

Abstract: Reservoir porosity is a critical parameter in the process of unconventional oil and gas resources assessment. It is difficult to determine the porosity of gas shale reservoir, so the large deviation will directly reduce the credibility of shale gas resources evaluation. However, there is no quantitative explanation for the accuracy of porosity measurement. In this paper, measurement uncertainty, an internationally recognized index, was used to evaluate the results of porosity measurement of gas shale plugs, and its impact on the credibility of shale gas resources was determined. The following conclusions are drawn: (1) the measurement uncertainty of porosity of shale plug is 1.76% ~ 3.12% in current measurement methods, part of which is too large to be acceptable. It is suggested that the measurement uncertainty should be added in the standard of helium gas injection porosity determine experiment, and the uncertainty should be less than 2.00% by using high-precision pressure gauge; (2) in order to reduce the risk of exploration and decision-making, attention should be paid to the large uncertainty (30% at least) of shale gas resources assessment results, sometimes corrections should be made base on the practicalities；(3) The pressure gauge with accuracy of 0.25% F.S. cannot meet the requirements of porosity measurement, and high-precision plug cutting method or high-precision bulk volume measurement method like 3D scanning method are recommended to effectively reduce the uncertainty of porosity; (4) The method and process for evaluating the measurement uncertainty of gas shale porosity could be referred for experiment quality assessment by other laboratories.

Key words: shale gas, resource assessment, porosity, measurement uncertainty

E-mail: tianhua86@petrochina.com.cn

1 Introduction

In recent years, unconventional petroleum exploration, especially shale gas, has drawn the interests of researchers all over the world (Curtis, 2002; Ewing, 2006; Hill et al., 2007; Li et al., 2013; Zou, 2014; Dong et al., 2018). Shale gas resource assessment has carried out by many institutions. As the huge amount of shale gas resources not only relates to the formulation of national energy development strategy, but also directly affects the exploration work of oil companies (Li Jianzhong et al., 2009; Zou et al., 2010, 2018; Ma et al., 2018). For basins with little drilling， the volumetric method is a commonly used resource assessment method, in which effective porosity (abbreviated as porosity) is the dominant parameter. Comparing with conventional reservoirs, there are a lot of nano-scale pore in tight reservoirs, which has complex pore-throat networks (Li Yanjun et al., 2013; Mahmood et al., 2018). One of the main characteristics of tight reservoirs is low porosity (less than 10% generally). Porosity of shale reservoirs is even less than 5%. The deviation of porosity measurement (Curtis et al., 2010; Hartmann et al., 2008, Xu Hao et al., 2015; Tang Xianglu, et al., 2016) will directly reduce

This article has been accepted for publication and undergone full peer review but has not been through the copyediting, typesetting, pagination and proofreading process, which may lead to differences between this version and the Version of Record. Please cite this article as doi: 10.1111/1755-6724.14287.

the credibility of shale gas resource assessment. In addition, the lower limit of porosity is also an important parameter for calculating shale gas reserves, which directly affects the productivity construction of oil companies, and this problem has gradually attracted the attention of researchers. How to evaluate he porosity measurement uncertainty of shale reservoir accurately has become an important problem. The conventional reservoir porosity testing methods (Bowker, 2007; Loucks et al., 2007; Sondergeld et al., 2010; Bustin et al., 2008) are used in the experiments. However, the measurement deviation caused by the particularity of shale is neglected and the quantitative description of the accuracy of porosity measurement is lacking, which seriously restricts the evaluation of the accuracy of shale resource.

Measurement errors are usually used to represent the difference between measured values and true values (Tian Hua et al., 2012; Chen Siyu et al., 2016), but true value itself is a quantity that needs to be recognized but cannot be accurately measured because of the existence of errors, which leads to logical confusion and quantitative difficulties in practical operation. Therefore, the concept of uncertainty is proposed to replace the concept of error. In 1993, seven international organizations, such as the International Organization for Standardization (ISO), jointly released the Guidelines for the Representation of Uncertainty in Measurement, which unified the concept of uncertainty and its mathematical processing methods. This standard was issued and recommended worldwide practice in 2005. Several scholars used uncertainty to evaluate the uncertainty of adsorption capacity of coal bed methane and shale gas (Goodman et al., 2004; Gensterblum et al., 2009; Gasparik et al., 2014). Uncertainty analysis was carried out by Ke Shizhen et al. (2007) on a sandstone samples with porosity of 17.3%. However, the uncertainty is less estimated as the high porosity of sandstone is different from that of shale reservoir samples. In this study, the uncertainty components under different experimental conditions are evaluated, and its influence on shale gas resource evaluation is quantitatively explained.

2 Geological Settings

The Lower Silurian Longmaxi Formation shale, with an area of about $12.82\times10^4 km^2$, is well developed and distributed in the eastern and southern parts of Sichuan basin, and the thickness is between 50 and 250m. This shale is lost because of erosion occurred in Leshan-Longnusi paleo-uplift in the western part of the basin (Ran Bo et al., 2016; Chen Fangwen et al., 2018; Zhang Yuanyin et al., 2018). The thickness of black shale in the whole basin is as much as 160m to 260 m, which increases gradually from west to east. The maximum thickness of black shale is about 260 m in Yibin city in the south of the basin (Fig. 1). The top burial depth of Longmaxi Formation is generally between 2000m and 3000m. In the northern part of Weiyuan area, the top boundary is nearly 4000m, and in the eastern part of the basin, the burial depth is more than 4000m.

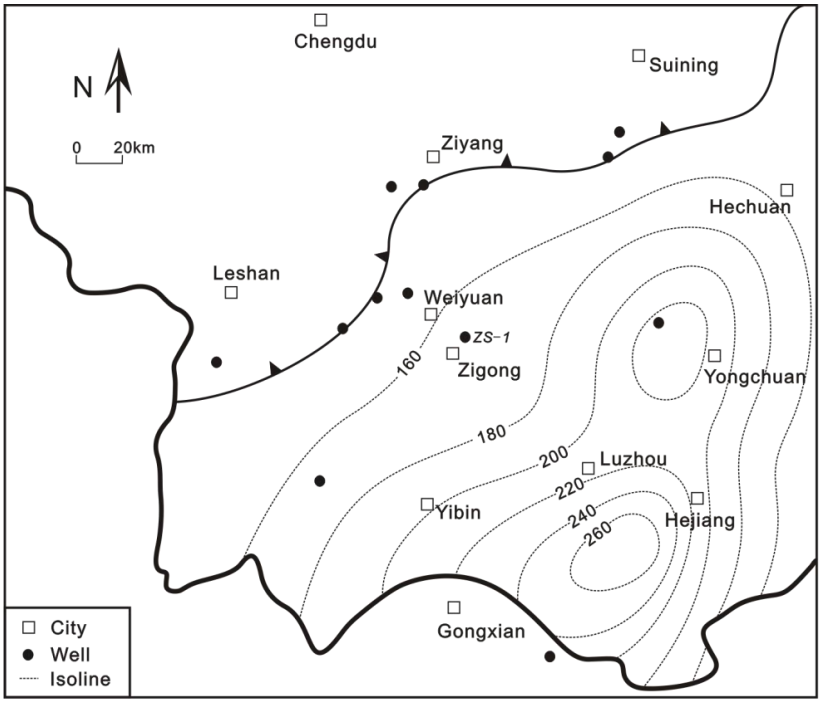

Fig. 1. Black shale thickness odistribution of Longmaxi Formation in southwest Sichuan basin.

3 Samples and Methods

3.1 Samples

Typical marine shale samples were selected from the shale gas reservoir in Sichuan basin, SW China. The samples are downhole core plugs of Lower Silurian Longmaxi Formation.

3.2 Helium injection method of porosity measurement

The process of measuring effective porosity of core plugs includes: (a) input helium at a certain pressure in the reference chamber, open the valves of the reference chamber and the sample chamber. (b) Fill the reference chamber gas into the sample chamber with known volume samples, measure the equilibrium pressure. (c) Measure the sample pore volume according to the variation of gas pressure (Fig. 2), and calculate the porosity (API, 1998； Tian Hua et al., 2012).

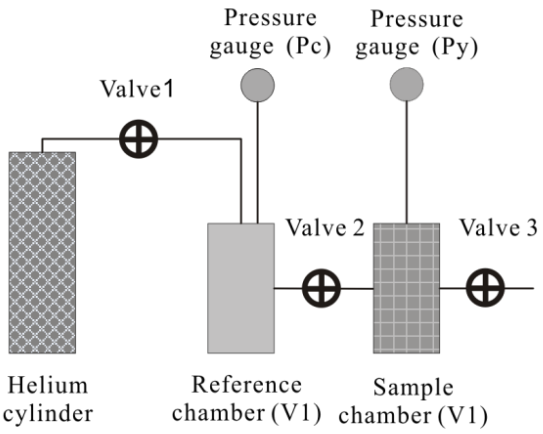

Fig. 2. Diagram of porosity measurement by helium injection method.

The specific steps of core plug porosity measurement are as follows:

Step 1: Measure the diameter *D* and length *L* of core plug with vernier calipers, and calculate the bulk volume *V*y (Eq. 1):

$$V_y = \frac{\pi \times D^2 \times L}{4} \quad (1)$$

Step 2: Empty the reference chamber, sample chamber and pipeline. The reference chamber is filled with standard blocks.

Step 3: Put the core plug into the sample chamber, record the volume of the standard block taken out (V_{b0}). Step 4: Close valve 1, valve 2, and valve 3.

Step 5: Open valve 1 and inject air into the reference chamber. The initial pressure is between 0.1 MPa and 0.9 MPa.

Step 6: Close valve 1 and record Pc and Py after the pressure gauge is stable.

Step 7: Open valve 2, and record Pcy after the pressure gauge is stable.

Step 8: Open valve 3, and the experiment is ended.

The bulk volume of core plug is V_y and the pore volume is V_k, which can be obtained from the Eq. of state of ideal gas.

$$P_c \times V_1 + P_y\left(V_2 + V_{b0} - V_y + V_k\right) = P_{cy}(V_1 + V_2 + V_{b0} - V_y + V_k) \quad (2)$$

Then,

$$V_{\mathrm{k}} = \frac{\mathrm{V_1(P_c - P_{cy})}}{\mathrm{P_{cy} - P_y}} - V_2 - V_{\mathrm{b0}} + V_{\mathrm{y}} \quad (3)$$

According to the definition of sample porosity, porosity is:

$$\phi = \frac{V_k}{V_y} \times 100\% \quad (4)$$

From Eq. 3 and 4,

$$\phi = \left(\frac{V_1\frac{(P_c - P_{cy})}{(P_{cy} - P_y)} - V_2 - V_{b0} + V_y}{V_y}\right) \times 100\% \quad (5)$$

D = diameter of core plug

L = length of core plug

V_{b0} = volume of standard block taken out

P_c = equilibrium helium pressure in reference chamber after closing valve 1

P_y = equilibrium atmospheric pressure in sample chamber after closing valve 1

P_{cy} = equilibrium helium pressure in sample chamber after closing valve 2

V_1 = volume of sample chamber

V_2 = volume of reference chamber

V_k = pore volume of core plug

V_y = bulk volume of core plug

ϕ = porosity of core plug

3.3 Measurement uncertainty

Uncertainty refers to the degree to which the measured value cannot be determined due to the existence of measurement errors in the experimental measurement results, indicating that the true value of the measured value exists in the evaluation of a certain range of values (Taylor et al., 1999; Ke Shizhen et al., 2007). Uncertainty reflects the reliability of measurement results. It can be understood as the error limit of a certain probability. Specifically, the error distribution associated with a certain confidence probability is a definite value, and the expression of uncertainty is more reasonable than the error.

The true value of measurement is objective, but it is uncertain. The measured results are usually expressed by the agreed true value; the true value is distributed in a certain confidence interval with a certain confidence probability (e.g. 95%); the half width of the confidence interval is the uncertainty of the measured results. The smaller the uncertainty is, the greater the reliability of measurement results.

3.3.1 Type A standard uncertainty

Uncertainty components that can be assessed by statistical methods (i.e. type A components) are named type A standard uncertainties. Type A uncertainty assessment is only applicable to statistical analysis of observation data obtained by laboratories, which is expressed by u_A.

3.3.2 Relative standard uncertainty

The quotient of standard uncertainty divided by the absolute value of the measurement result is relative standard uncertainty, which is dimensionless and expressed by u_{rel}.

3.3.3 Type B standard uncertainty

Uncertainty components that cannot be evaluated by statistical methods (i.e. type B components) are named type B standard uncertainties. Standard uncertainties are assessed using a different method from statistical analysis of observation data, which is usually expressed by u_B.

3.3.4 Combined standard uncertainty

The arithmetic square root obtained by adding the uncertainties of type A and type B, which is expressed by u_c.

3.3.5 Expanded Uncertainty

Expanded uncertainty refers to the interval width in which the measured value exists with a certain confidence probability. The Expanded uncertainty U can be obtained by multiplying the combined standard uncertainty by a factor (called inclusion factor). Uncertainty evaluation is closely related to measurement process. The goal of uncertainty measurement is to determine the value of measurement and give the uncertainty of the value, which includes the following five steps (Fig. 3):

(1) Overview of measurement methods: Clear and accurate description of measurement process, including method name, sample decomposition and measuring instruments and measurement parameters, etc. It is closely related to the evaluation of parameters and measurement uncertainty, which give a clear understanding of the source of measurement uncertainty.

(2) Establishing mathematical models: according to measurement methods, establish the functional relationship between output (measured y) and input (Xi), that is, the calculation Eq. of measured y is listed, and the quantitative relationship between Y and input (Xi) is clarified.

(3) Identification of measurement uncertainty sources: the sources of measurement uncertainty are analyzed and the main influencing factors are found according to measurement methods and measurement conditions. The influence of uncertainty is not only directly related to the input (xi), but also to the indirect factors that affect the input.

(4) Assessment of standard uncertainty: the uncertainty of the output (measured Y) depends on the uncertainty of the input (Xi) estimates. For this reason, the type A and type B standard uncertainties are evaluated respectively, and the expanded uncertainty is finally obtained.

(5) Report of measurement uncertainty.

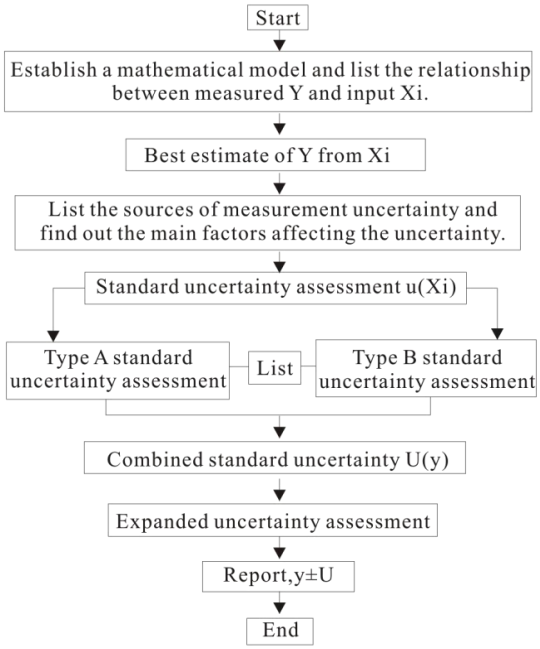

Fig. 3. The general steps of standard uncertainty assessment.

4 Results

Each uncertainty component of the analysis is quantified and transformed into standard uncertainty. The uncertainties of each identified potential source are estimated by direct measurement data or derived from theoretical analysis. The evaluation includes type A uncertainty component and type B uncertainty component, and then calculates the combined uncertainty and expanded uncertainty.

The type A uncertainty component is affected by the variation of sample diameter, length, pressure, atmospheric pressure and temperature in repetitive measurement (Fig. 4). These factors can be evaluated by repetitive test. Type B uncertainty components include pressure gauge, sample volume, standard block volume, volume of reference chamber, volume of sample chamber, etc.

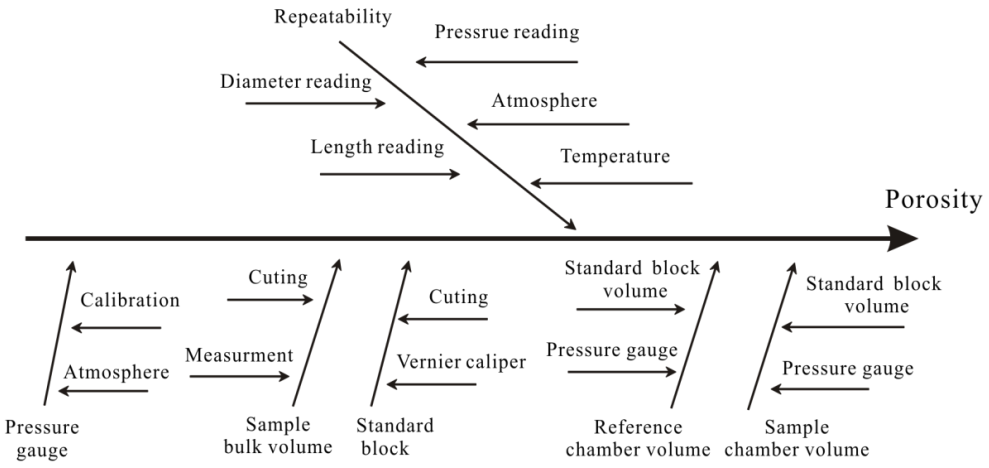

Fig. 4. Causality diagram of uncertainty in porosity measurement.

4.1 Type A uncertainty assessment

The type A uncertainty was assessed based on the standard deviation calculated by Bessel's formula. Three shale samples were selected to measure porosity independently for ten times, and the condition of repeatability was: (1) the same measuring procedure; (2) the same measuring personnel; (3) the same measuring equipment under the same conditions; (4) the same measurement equipment; (4) the same location; (5) Repeated measurement in a short time. The standard deviation sj of each group of experiments is:

$$s_j = \sqrt{\frac{\sum_{i=1}^{10}\left(X_i - \bar{X}\right)^2}{10-1}} \tag{6}$$

Due to the independent measurement of three groups of samples (Table 1), the standard uncertainty of measurement (u_A) equals to the standard deviation (s_P). The type A uncertainty (u_A) of porosity measurement is 0.218%, according to Eq. 7.

$$s_p = \sqrt{\frac{1}{3}\sum_{j=i}^{3} s_j^{\,2}} \tag{7}$$

Table 1 Repeated measurement results and standard deviations

x_i	Sample b0(%)	Shale b5 (%)	Shale J-3 (%)
x_1	-0.04	5.83	1.10
x_2	-0.18	6.33	1.05
x_3	-0.01	6.12	1.05
x_4	0.00	5.71	0.84
x_5	-0.16	5.77	0.91
x_6	-0.23	5.33	0.93
x_7	-0.17	5.74	0.97
x_8	-0.18	5.25	0.95
x_9	-0.18	5.82	1.04
x_{10}	-0.16	6.25	1.02
Standard deviation s_j	0.093	0.353	0.098

Note: Sample b0 is a solid stainless steel cylinder with theoretical porosity of 0%.

4.2 Type B uncertainty assessment

Type B uncertainty assessment is usually conducted based on previous observation data, relevant information or data, include: (a) data from previous measurements or assessments; (b) knowledge of relevant technical data and characteristics of measuring instruments; (c) technical documentation provided by manufacturers; (d) data from calibration and verification certificates, grade or level of accuracy; (e) uncertainty from manuals or references; (f) the repeatability limit or reproducibility limit R given by standards. The standard uncertainties of pressure gauge, bulk volume of core plug, standard block volume, reference chamber volume and sample chamber volume are calculated.

4.2.1 Pressure gauge

The standard uncertainty components introduced by the pressure gauge are reference chamber pressure $u_B(P_c)$ and sample chamber equilibrium pressure $u_B(P_{cy})$. The pressure gauge accuracy in laboratories is commonly 0.25% or 0.1% of the full scale. Few laboratories use high accuracy pressure gauge with the accuracy of 0.03% of the full scale. As the standard deviations follow uniform distribution, so the standard uncertainties of pressure gauge with different accuracy are 0.0025/3=0.00144MPa, 0.0010/3=0.00058MPa and 0.0003/3=0.00017 MPa respectively.

The standard uncertainty component introduced by barometer for measuring atmospheric pressure in sample chamber is $u_B(P_y)$. According to the verification certificate of barometer, its maximum allowable error is ±0.0002 MPa, which is considered to follow uniform distribution. The standard uncertainty of $u_B(P_y)$ is $0.0002/\sqrt{3}$=0.00012MPa.

4.2.2 Bulk volume of core plug

The bulk volume of core plug is usually measured by vernier calipers, and the error mainly comes from core plug cutting process and vernier caliper measurement.

Shale core plugs are usually difficult to be cut into ideal cylinders while measuring the bulk volume, which brings measurement uncertainties. Like the upper and lower sections are not parallel, the height of the cylinder is not uniform, the cylinder is not straight, the cylinder surface of the sample is incomplete, uneven, cracked, and the upper and lower ends are uneven (Fig. 5). The error limits of length and diameter were counted as ±0.025 cm and ±0.013 cm repectively (Chen Siyu et al., 2016). According to uniform distribution, the standard uncertainty of length and diameter are $u(L)_1=0.013/\sqrt{3}$=0.0075cm and $u(D)_1=0.025/\sqrt{3}$=0.0144cm respectively. Besides, diameter (and length) is measured by vernier calipers, and its maximum allowable error of vernier calipers is ±0.0020 cm. According to uniform distribution, its standard uncertainty $u(d)_1$ is 0.0020/3=0.0012 cm. The key laboratory of basin structure and hydrocarbon accumulation of CNPC has developed a high-precision 3D scanning method for measuring sample volume (Chen Siyu et. al., 2016). The volume measurement error produced by this method is independent of the cutting accuracy of the sample, but only related to the accuracy of the instrument itself. Statistical results show that the error limit is ±0.105 cm3. According to uniform distribution, the standard uncertainty is $u_B(V_y)=0.105/\sqrt{3}$=0.060cm^3.

In summary, the uncertainty component of sample diameter measurement is $u(D)=\sqrt{u^2(d)_1 + u^2(D)_1}$ =0.0144cm, and the uncertainty component of sample length measurement is $u(L)=\sqrt{u^2(d)_1 + u^2(L)_1}$ =0.0075cm. According to Eq. 1, the uncertainty component of bulk volume measurement is $u_B(V_y)=\sqrt{2u^2(D) + u^2(L)}$ =0.121 cm^3.

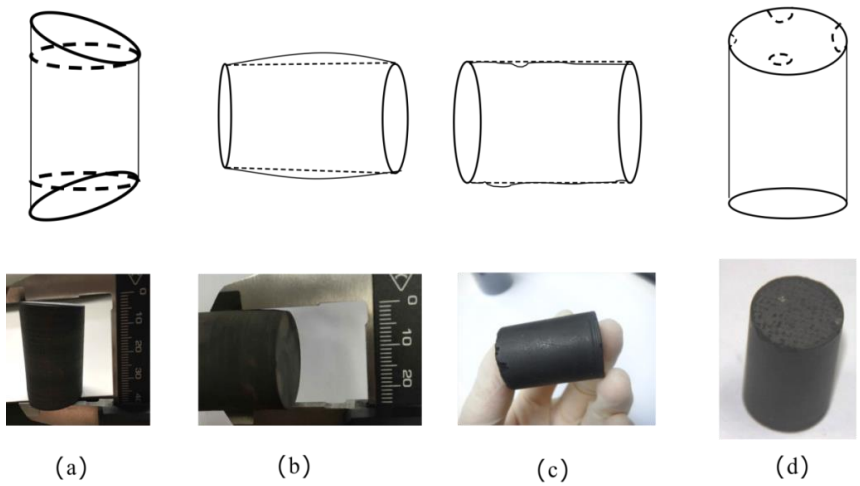

Fig. 5. Main types of shape defects while core plug cutting (Chen Siyu et al., 2016).

4.2.3 Standard block volume taken out

The standard block taken out is a solid stainless steel cylinder. The uncertainty component mainly comes from measurement of diameter and length with vernier caliper. The maximum allowable error of the vernier caliper is (±0.0020

cm). According to uniform distribution, its standard uncertainty $u(d)_1$ is 0.0020/3=0.0012 cm. According to Eq. 1, the uncertainty component of standard block volume taken out measurement is $u_B(V_{b0})=\sqrt{2u^2(d)_1+u^2(d)_1}$ =0.0147 cm^3.

4.2.4 Volume of reference chamber and sample chamber

According to the instrument instructions, the volume accuracy of reference chamber and sample chamber is 0.005cm^3 and 0.015cm^3 respectively. Referring to uniform distribution, the standard uncertainty of the volume of reference chamber and sample chamber is $u_B(V_1)=0.005/\sqrt{3}=0.003cm^3$ and $u_B(V_1)=0.005/\sqrt{3}=0.003cm^3$ respectively.

4.2.5 Type B standard uncertainty

Porosity measurement was conducted on the sl-2 black shale collected from Longmaxi Formation. The porosity measurement result is 2.14%. The pressure gauge accuracy is 0.1% of the full scale. The bulk volume is measured by vernier caliper. The uncertainty components are shown in Table 2. According to Eq. 3, the calculation process of Type B standard uncertainty of pore volume V_k is as follows:

$$u_B(V_k)=u_B\left(V_1\frac{P_c-P_{cy}}{P_{cy}-P_y}-V_2-V_{b0}+V_y\right)=\sqrt{u_B^2\left(V_1\frac{P_c-P_{cy}}{P_{cy}-P_y}\right)+u_B^2(V_2)+u_B^2(V_{b0})+u_B^2(V_y)} \quad (8)$$

where,

$$u_B\left(V_1\frac{P_c-P_{cy}}{P_{cy}-P_y}\right)=u_{rel}\left(V_1\frac{P_c-P_{cy}}{P_{cy}-P_y}\right)\times V_1\frac{P_c-P_{cy}}{P_{cy}-P_y} \quad (9)$$

$$u_{rel}\left(V_1\frac{P_c-P_{cy}}{P_{cy}-P_y}\right)=\sqrt{u_{rel}^2(P_c-P_{cy})+u_{rel}^2(P_{cy}-P_y)+u_{rel}^2(V_1)} \quad (10)$$

$$u_{rel}(P_c-P_{cy})=\frac{u_B(P_c-P_{cy})}{(P_c-P_{cy})} \quad (11)$$

$$u_{rel}(P_{cy}-P_y)=\frac{u_B(P_{cy}-P_y)}{(P_{cy}-P_y)} \quad (12)$$

$$u_{rel}(V_1)=\frac{u_B(V_1)}{(V_1)} \quad (13)$$

$$u_B(P_c-P_{cy})=\sqrt{u^2(P_c)+u^2(P_{cy})} \quad (14)$$

$$u_B(P_{cy}-P_y)=\sqrt{u^2(P_{cy})+u^2(P_y)} \quad (15)$$

From Eq. 5, Type B standard uncertainty of porosity ϕ is:

$$u_{rel}(\phi)=\sqrt{u_{rel}{}^2(V_k)+u_{rel}{}^2(V_y)} \quad (16)$$

Where,

$$u_{rel}(V_k)=\frac{u_B(V_k)}{(V_k)} \quad (17)$$

$$u_{\mathrm{rel}}(V_{\mathrm{y}})=\frac{u_{\mathrm{B}}(V_{\mathrm{y}})}{(V_{\mathrm{y}})} \tag{18}$$

So,

$$u_{\mathrm{B}}\ (\phi)=u_{\mathrm{rel}}\ (\phi)\times\phi \tag{19}$$

Table 2 Summary of uncertainty components

Uncertainty component (u)	V_2	V_1	V_{b0}	V_y	P_c	P_y	P_{cy}	V_k	ϕ
Unit	cm^3	cm^3	cm^3	cm^3	MPa	MPa	MPa	cm^3	%
Standard uncertainty (u_B)	0.009	0.003	0.0147	0.121	0.00058	0.00012	0.00058	0.132	0.92
Value	15.347	13.366	19.306	14.32	0.963	0.098	0.438	0.306	2.14
Relative uncertainty (u_{rel})	0.00059	0.00022	0.00076	0.00848	0.00060	0.00122	0.00132	0.431	0.43

4.3 Combined standard uncertainty and expanded uncertainty

Combined standard uncertainty is calculated through type A standard uncertainty and type B standard uncertainty (Eq. 20).

$$u_{\mathrm{c}}(\phi)=\sqrt{u_{\mathrm{A}}^2+u_{\mathrm{B}}^2} \tag{20}$$

In the 95% confidence interval, the expanded uncertainty is

$$U=k\times u\ (\phi)=2u_{\mathrm{c}}\ (\phi)\ =1.90\% \tag{21}$$

Where k is inclusion factor, k = 2.

The porosity value of this sample considering uncertainty is 2.14%±1.90% (Table 3). The expanded uncertainty is as high as 1.90%, which almost equals to the measured value. The measured value is in the range of 0.24%~4.04% with 95% probability. The high expanded uncertainty causes the low reliability of the porosity measurement although the type A uncertainty is low (0.22%).

Table 3 Summary of porosity measurement uncertainty

Porosity measurement uncertainty	Unit	Value
Type A standard uncertainty (u_A)	%	0.22
Type A standard uncertainty (u_B)	%	0.92
Combined uncertainty (u_c)	%	0.95
Expanded uncertain (U)	%	1.90

4.4 Method validity

In order to verify the validity of uncertainty assessment, twelve more times experiments were made on the same sample (sl-2). Unlike the type A uncertainty repeatability measurement, several experimenters were selected to do the measurements in different times. The statistical results show that (Table 4), the mathematical average is 2.17%, and the maximum deviation is as large as 1.65%, which is close to the result of expanded uncertainty assessment. The tested result

is slightly lower than that of expanded uncertainty that is on the hypothesis of infinite measurement, which confirms the validity of this uncertainty assessment method.

Table 4 Shale porosity measurement of sl-2 sample

No.	1	2	3	4	5	6	7	8	9	10	11	12
Value (%)	0.52	0.86	0.98	1.39	1.73	1.97	2.34	2.65	2.97	3.23	3.56	3.82

5 Discussions

In order to quantitatively evaluate the expanded uncertainty of porosity under different measurement conditions, and improve the accuracy of shale porosity measurement, it is necessary to quantitatively analyze the influence factors, such as rock compactness (i.e. porosity scale), bulk volume and pressure gauge accuracy. The influence of expanded uncertainty on the shale gas resources credibility was also analyzed.

5.1. Influencing factors on porosity uncertainty

Porosity measurements were carried out on four shales with different porosity (0.59%~6.02%), and each sample was tested under five different conditions. Twenty experiments are conducted and the expanded uncertainty under 95% confidence interval is evaluated (Table 5). The expanded uncertainty ranges between 0.88% and 3.12%, which is mainly affected by measuring instruments. It is shown that the uncertainty of the same instrument almost invariable. With the decrease of porosity, the maximum uncertainty can reach nearly two times of the measured value (198%), leading to the serious low credibility of porosity measurement of tight reservoir samples (Fig. 6).

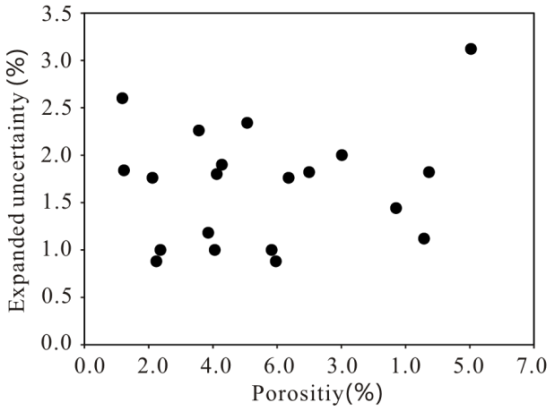

Fig. 6. Expanded uncertainty of shales with different porosity.

The accuracy of pressure gauge has a great influence on expanded uncertainty, which range from 2.26% to 3.12% by using the pressure gauge with accuracy of 0.25% F.S. The expanded uncertainty of sl-3 sample is the smallest (2.26%) , which accounts for 127% of the measured value, larger than the measured porosity(1.78%). It is found that the uncertainty caused by the pressure gauge with accuracy of 0.25% F.S. is too large to meet the requirements of shale porosity measurement. Compared with the pressure gauge with accuracy of 0.25% F.S., the pressure gauge with accuracy of 0.1% F.S. has significant advantages, and the expanded uncertainty is greatly reduced to 1.00%~2.00%. The uncertainty decreases slightly while pressure gauge accuracy is 0.03%F.S. compared with the pressure gauge measurement with accuracy 0.1%F.S., which indicates that improving the pressure gauge accuracy alone cannot effectively reduce the expanded uncertainty (Fig. 7).

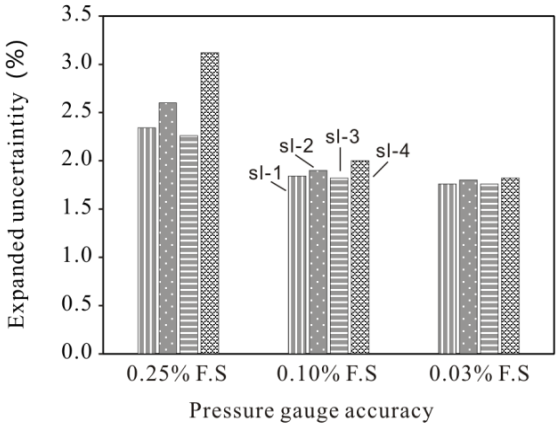

Fig. 7. The influence of pressure gauge accuracy on expanded uncertainty.

The uncertainty of porosity measurement can be significantly reduced by using 3D scanning method to test sample bulk volume compared with vernier caliper method for the pressure gauge accuracy both of 0.1% F.S. and 0.03% F.S. For example, the expanded uncertainty of porosity measurement is 1.50%~2.00% when using vernier caliper to measure sample bulk volume, whereas most expanded uncertainty decrease to less than 1.14% when using 3D scanning method to measure sample bulk volume (Fig. 8). In order to obtain the most reliable porosity data, it is necessary to further develop 3D scanning method for sample bulk volume measurement while using the highest precision pressure gauge as possible.

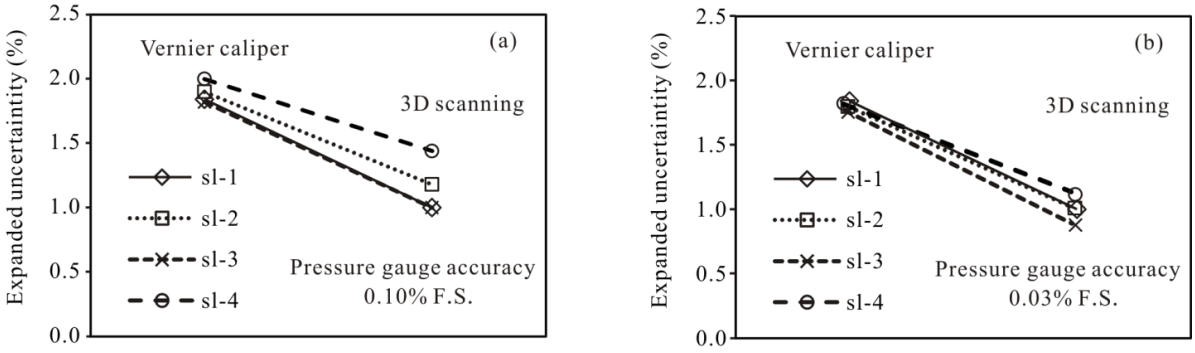

Fig. 8. Comparison of porosity measurement expanded uncertainty between 3D scanning method and vernier caliper method.

(a) Pressure gauge accuracy is 0.1%F.S; (b) Pressure gauge accuracy is 0.03%F.S.

5.2 Influence of porosity uncertainty on resource assessment

The volumetric gas resource assessment method is most commonly used in low exploration basins. Shale gas is composed of free gas and adsorbed gas (Zhao Wenzhi et al., 2016). Porosity mainly affects free gas content. The volumetric method is mainly based on the following formulas for calculating the amount of shale gas geological resources:

$$G = G_{\mathrm{f}} + G_{\mathrm{s}} = \frac{0.01 \cdot A \cdot h \cdot \Phi \cdot S_{\mathrm{g}}}{B_{\mathrm{g}}} + 0.01 \cdot A \cdot h \cdot \rho \cdot C_{\mathrm{s}} \tag{22}$$

Where,

G = shale gas geological resources,$10^8 \times m^3$;

G_f = free gas geological resource,$10^8 \times m^3$;

Gs = adsorbed gas geological resource, $10^8 \times m^3$;

A = shale reservoir area, km^2;

h = shale reservoir thickness, m;

S = shale gas saturation, 60%;

Φ = shale reservoir porosity, *%*;

B_g = formation factor, 0.0046, dimensionless;

ρ= shale reservoir density, $2.5 g/m^3$;

C_s = adsorbed gas content, $1.05 m^3/t$.

Table 5 Shale porosity expanded uncertainty under five different measurement conditions

No.	Sample	L (cm)	D (cm)	V_y (cm^3)	P_c (MPa)	P_y (MPa)	P_{cy} (MPa)	Sample bulk volume measure method	Pressure gauge accuarcy(MPa)	ϕ (%)	u_C (%)
1	sl-1	3.232	2.526	16.197	0.991	0.098	0.472	vernier caliper	0.0025	2.53	2.34
2	sl-1	3.232	2.526	16.197	0.953	0.098	0.456	vernier caliper	0.0010	0.62	1.84
3	sl-1	3.232	2.526	16.197	0.9964	0.098	0.4356	vernier caliper	0.0003	1.06	1.76
4	sl-1	/	/	16.763	0.9583	0.098	0.4269	3D scanning	0.0003	1.12	0.88
5	sl-1	/	/	16.763	0.964	0.098	0.466	3D scanning	0.0010	1.18	1.00
6	sl-2	2.853	2.536	14.411	0.958	0.098	0.445	vernier caliper	0.0025	0.59	2.60
7	sl-2	2.853	2.536	14.411	0.963	0.098	0.438	vernier caliper	0.0010	2.14	1.90
8	sl-2	2.853	2.536	14.411	0.9623	0.098	0.4046	vernier caliper	0.0003	2.06	1.80
9	sl-2	/	/	14.468	0.9253	0.098	0.3920	3D scanning	0.0003	2.03	1.00
10	sl-2	/	/	14.468	0.956	0.098	0.437	3D scanning	0.0010	1.93	1.18
11	sl-3	3.353	2.537	16.950	0.978	0.098	0.475	vernier caliper	0.0025	1.78	2.26
12	sl-3	3.353	2.537	16.950	0.965	0.098	0.464	vernier caliper	0.0010	3.50	1.82
13	sl-3	3.353	2.537	16.950	0.9675	0.098	0.4287	vernier caliper	0.0003	3.18	1.76
14	sl-3	/	/	16.909	0.9432	0.098	0.4194	3D scanning	0.0003	2.98	0.88
15	sl-3	/	/	16.909	0.987	0.098	0.474	3D scanning	0.0010	2.91	1.00
16	sl-4	2.569	2.518	12.793	0.908	0.098	0.407	vernier caliper	0.0025	6.02	3.12
17	sl-4	2.569	2.518	12.793	0.935	0.098	0.411	vernier caliper	0.0010	4.01	2.00
18	sl-4	2.569	2.518	12.793	0.916	0.098	0.4790	vernier caliper	0.0003	5.37	1.82

19	sl-4	/	/	12.808	0.894	0.098	0.4690	3D scanning	0.0003	5.29	1.12
20	sl-4	/	/	12.808	0.854	0.098	0.3800	3D scanning	0.0010	4.85	1.44

The Longmaxi Formation is mainly a set of shallow-deep water shelf faces deposits, consisting of deep gray, black silt shale, organic shale, siliceous shale and argillaceous siltstone, etc (Dong Dazhong et al., 2018). The Longmaxi Formation distributes continuously except for the strata erosion in the western part of the basin. Changning area in southern Sichuan basin is a successful shale gas production area (Cao Taotao et al., 2015; Jiao Kun et al., 2017), the exploration area of which is about $1.42\times10^{4}km^{2}$ with the thickness of black shale of 80 m in average. The burial depth of Longmaxi shale is 2500m in average. The shale reservoir density is $2.5g/m^{3}$, and adsorbed gas content is $1.05\ m^{3}/t$.

The shale gas content of Longmaxi shale in south Sichuan basin is $3.40m^{3}/t$, in which the free gas content is $2.35m^{3}/t$. The shale gas geological resource assessment result is $9.65\times10^{12}m^{3}$, and the gas concentration is $6.8\times10^{8}m^{3}/km^{2}$(Eq. 22). According to the porosity measurement expanded uncertainty (±1.90%), the uncertainty of shale gas geological resource in this area is $\pm2.81\times10^{12}m^{3}$, accounting for 30% of the total geological resources (Fig. 9), which is a large proportion of shale gas resources with a low level of confidence. This resource assessment result will bring great risks if it is used as the basis of gas field exploration and development.

It is assessed that the geological resource of shale gas in China is $134.42\times10^{8}m^{3}$ and the recoverable resources is $25.08\times10^{8}m^{3}$ by the ministry of land and resources. The uncertainty of porosity directly leads to the low reliability of shale gas resources assessment. The uncertain amount of geological resources and exploitable resources are $40\times10^{8}m^{3}$ and $7.5\times10^{8}m^{3}$ respectively, accounts for about 30% of their original amount. In order to reduce the risk of exploration and decision-making, attention should be paid to the large uncertainty (30% at least) of shale gas resources assessment results. It is all known that the potential of shale gas resources in China is huge, although the results released by different institutions are inconsistent (Jarvie et al., 2007; Zou Caineng et al., 2016; Li Yufeng et al., 2018; Zhai Gangyi et al., 2018). It is suggested that the reservoir porosity uncertainty should be taken into account in the application of shale gas resources evaluation, and sometimes corrections should be made base on the practicalities.

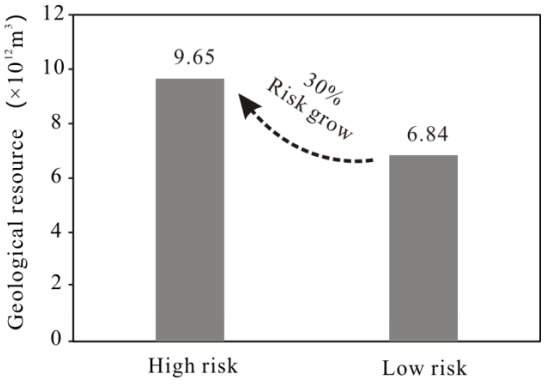

Fig. 9. Shale gas geological resource assessment results of Changning area, south Sichuan basin.

6 Conclusions

(1) This paper establishes a method for evaluating the uncertainty of porosity, which could be referred for experiment quality assessment by other laboratories.

(2) The expanded uncertainty of shale plug porosity measurement between 1.76% and 3.12% in current measurement methods, part of which is too large to be acceptable. It is unreasonable to use repetitive measurement only to express data quality. It is suggested that the measurement uncertainty should be added in the standard of helium gas injection porosity determine experiment, and the uncertainty should be less than 2.00% by using high-precision pressure gauge.

(3) The pressure gauge accuracy, the regularity of core plug bulk volume of, and its measurement method are the key factors affecting the uncertainty of porosity measurement. The pressure gauge with accuracy of 0.25% F.S. cannot meet the requirements of porosity measurement. When the pressure gauge accuracy is higher than 0.1% F.S., plug bulk volume is the dominant factor affecting the expanded uncertainty, which decrease to less than 1.14% when using 3D scanning method to measure sample bulk volume. it is necessary to further develop 3D scanning method for sample bulk volume measurement or high-precision bulk volume cutting method, which can effectively reduce the uncertainty of porosity measurement.

(4) The large uncertainty of shale reservoir porosity caused low credibility of shale gas geological resource assessment. In order to reduce the risk of exploration and decision-making, attention should be paid to the large uncertainty (30% at least) of shale gas resources assessment results, sometimes corrections should be made base on the practicalities.

Acknowledgements

This work is granted by the National Science and Technology Major Project of China (Grant No. 2016ZX05003-002), the National Key R&D Program of China (Grant No. 2017YFC0603101); the Strategic Priority Research Program of the Chinese Academy of Sciences (Grant No. XDA14010403) and the Science and Technology Programe of RIPED, PetroChina (Grant No. YGJ2019-05).

References

American petroleum institute, 1998. *Recommended practices for core analysis* (2nd ed.). Washington, D.C: API Publishing Services, 5-11.

Bowker K. A., 2007. Barnett Shale gas production, Fort Worth Basin: Issues and discussion. *AAPG Bulletin*, 91(4): 523–533.

Bustin R. M., Bustin A. M. M., Cui X., Ross D.J.K. and Murthy V.S., 2008. Impact of shale properties on pore structure and storage characteristics. *SPE Shale Gas Production Conference*, Fort Worth, Texas, USA.

Cao Taotao, Song Zhiguang, Wang Sibo, Cao Xinxing, Li Yan and Xia Jia, 2015. Characterizing the pore structure in the Silurian and Permian shales of the Sichuan Basin, China. *Marine & Petroleum Geology*, 61:140–150.

Chen Fangwen, Lu Shuangfang and Ding Xue, 2018. Pore Types and Quantitative Evaluation of Pore Volumes in the Longmaxi Formation Shale of Southeast Chongqing, China. *Acta Geologica Sinica* (English Edition),92(01):342–353.

Chen Siyu, Tian Hua, Liu Shaobo, Li Caixi, Hao Jiaqing and Zheng Yongping, 2016. Influence of bulk volume measurement on porosity error in tight reservoir core plug analysis. *Petroleum Geology and Experiment*, 38:850-856 (in Chinese with English abstract).

Curtis J. B., 2002. Fractured Shale-Gas Systems. *AAPG Bulletin*, 86(11): 1921–1938.

Curtis M. E., Ambrose R. J. and Sondergeld C.H., 2010. Structural characterization of gas shales on the micro-and nano-scales. *Canadian Unconventional Resources and International Petroleum Conference*, Calgary, Alberta, Canada.

Dong Dazhong, Shi Zhensheng, Sun Shasha, Guo Changmin, Zhang Chenchen, Guo Wen, Guan Quanzhong, Zhang Mengqi, Jiang Shan, Zhang Leifu, Ma Chao, Wu Jin, Li Ning and Chang Yan, 2018. Factors controlling microfractures in black shale: A case study of Ordovician Wufeng Formation-Silurian Longmaxi Formation in Shuanghe Profile,Changning area, Sichuan Basin, SW China. *Petroleum Exploration & Development*, 2018,45(05): 818–829.

Ewing T. E.,2006. Mississippian Barnett Shale, Fort Worth basin, north-central Texas: Gas-shale play with multi-trillion cubic foot potential: Discussion. *AAPG Bulletin*, 90(6): 963–966.

Gasparik M., Rexer T. F. T., Aplin A. C., Billemont P. , Weireld G. D. , Gensterblum Y., Henry M., Krooss B. M. Liu S., Ma X., Sakurovs R., Song S., Staib G. Thomas K. M., Wang S. and Zhang T., 2014. First international inter-laboratory comparison of high-pressure CH4, CO2, and C2H6, sorption isotherms on carbonaceous shales. *International Journal of Coal Geology*, 132:131–146.

Gensterblum Y., Hemert P. V., Billemont P.B., Busch A., Charriére D., Li D., Krooss B. M., Weireld G., Prinz D., Wolf K.-H.A.A., 2009. European inter-laboratory comparison of high pressure CO2 sorption isotherms. I: Activated carbon. Carbon, 47(13):2958–2969.

Goodman A. L., Busch A, Duffy G. J., Fitzgerald J. E. , Gasem K., Gensterblum Y., Krooss B. M., Levy J., Ozdemir E., Pan Z., Schroeder K. and Sudibandriyo M., 2004. An inter-laboratory comparison of CO2 isotherms measured on Argonne premium coal samples. *Energy & Fuels*, 18(4):1175–1182.

Hartmann A, Pechnig R and Clauser C., 2008. Petrophysical analysis of regional-scale thermal properties for improved simulations of geothermal installations and basin-scale heat and fluid flow. International Journal of Earth Sciences, 97(2):421–433.

Hill R. J., Jarvie D M, Zumberge J, Henry M. and Pollastro R.M., 2007. Oil and gas geochemistry and petroleum systems of the Fort Worth Basin. *AAPG Bulletin*, 91(4): 445–473.

Jarvie D. M., Hill R. J., Ruble T. E. and Pollastro R.M., 2007. Unconventional shale-gas systems: The Mississippian Barnett Shale of north-central Texas as one model for thermogenic shale-gas assessment. *AAPG Bulletin*, 91(4): 475–499.

Jiao Kun, Ye Yuehao, Liu Shugen, Ran Bo, Deng Bin, Li Zhiwu, Li Jinxi, Yong Ziquan and Sun Wei, 2017. Characterization and Evolution of Nanoporosity in Superdeeply Buried Shales: A Case Study of the Longmaxi and Qiongzhusi Shales from MS Well #1,

North Sichuan Basin, China. *Energy & Fuels*, 2017, 32(1):191–203.

Ke Shizhen, He Yicheng and Wang Jieyi, 2007. Uncertainty analysis of gas porosity measurement of rock. *Acta Merologica Sinica*, 28:177–179 (in Chinese with English abstract).

Li Jianzhong, Dong Dazhong, Chen Gengsheng, Wang Shiqian and Cheng Keming, 2009. Prospects and strategic position of shale gas resources in China. *Natural Gas Industry*, 5:11–16 (in Chinese with English abstract).

Li Yanjun, Feng Yuanyuan, Liu Huan, Zhang Liehui and Zhao Shengxian, 2013. Geological characteristics and resource potential of lacustrine shale gas in the Sichuan Basin,SW China. *Petroleum Exploration & Development*, 40(4):454–460.

Li Yanjun, Liu Huan, Zhang Liehui, Lu Zonggang, Li Qirong and Huang Yongbin, 2013. Lower limits of evaluation parameters for the lower Paleozoic Longmaxi shale gas in southern Sichuan Province. *Science China(Earth Sciences)*, 7:1088–1095.

Li Yufeng, Sun Wei, Liu Xiwu, Zhang Dianwei, Wang Yanchun and Liu Zhiyuan, 2018. Study of the relationship between fractures and highly productive shale gas zones, Longmaxi Formation, Jiaoshiba area in eastern Sichuan. *Petroleum Science*, 15(03):498–509.

Loucks R G, Ruppel S C., 2007. Mississippian Barnett Shale: Lithofacies and depositional setting of a deep-water shale-gas succession in the Fort Worth Basin, Texas. *AAPG Bulletin*, 91(4): 579–601.

Ma Yongsheng, Cai Xunyu and Zhao Peirong, 2018. China's shale gas exploration and development: Understanding and practice. *Petroleum Exploration & Development*, 45(04): 589–603.

Mahmood M F, Ahmad Z and Ehsan M. Total organic carbon content and total porosity estimation in unconventional resource play using integrated approach through seismic inversion and well logs analysis within the Talhar Shale, Pakistan. *Journal of Natural Gas Science & Engineering*, 2018, 52(April):13–24.

Ran Bo, Liu Shugen, Luba JANSA, Sun Wei, Yang Di, Wang Shiyu,Ye Yuehao, Christopher Xiao, Zhang Jian, Zhai Cangbo, Luo Chao and Zhang Changjun, 2016. Reservoir Characteristics and Preservation Conditions of Longmaxi Shale in the Upper Yangtze Block,South China[J].*Acta Geologica Sinica* (English Edition),90(06):2182–2205.

Sondergeld C. H., Ambrose R. J., Rai C. S. and Moncrieff J., 2010. Micro-structural studies of gas shales. *SPE Unconventional Gas Conference*, Pittsburgh, Pennsylvania, USA.

Tang Xianglu, Jiang Zhenxue, Jiang Shu and Li Zhuo, 2016. Heterogeneous nanoporosity of the Silurian Longmaxi Formation shale gas reservoir in the Sichuan Basin using the QEMSCAN, FIB-SEM, and nano-CT methods. *Marine & Petroleum Geology*, 78:99–109.

Taylor R P, Mcclain S T and Berry J T., 1999. Uncertainty analysis of metal-casting porosity measurements using Archimedes" principle. *Cast Metals*, 11(4):247–257.

Tian Hua, Zhang Shuichang, Liu Shaobo, Ma Xingzhi and Zhang Hong, 2012. Parameter optimization of tight reservoir porosity determination. *Petroleum Geology and Experiment*, 34:334–339 (in Chinese with English abstract).

Xu Hao, Tang Dazhen, Zhao Junlong and Li Song, 2015. A precise measurement method for shale porosity with low-field nuclear magnetic resonance: A case study of the Carboniferous–Permian strata in the Linxing area, eastern Ordos Basin, China. *Fuel*, 143:47–54.

Zhai Gangyi，Wang Yufang and Zhou Zhi, 2018. Exploration and research progress of shale gas in China. *China Geology*, 2:257−272.

Zhang YuanYin, Jin ZhiJun, Chen YeQuan, Liu XiWu, Han Lei and Jin Wujun, 2018. Pre-stack seismic density inversion in marine shale reservoirs in the southern Jiaoshiba area, Sichuan Basin, China. *Petroleum Science*,15(03):484–497.

Zhao Wenzhi, Li Jianzhong, Yang Tao, Wang Shufang and Huang Jinliang, 2016. Geological difference and its significance of marine shale gases in South China. *Petroleum Exploration & Development*, 43(4):547–559.

Zou Caineng, 2014. *Unconventional petroleum Geology*. Beijing: Geology Press.

Zou Caineng, Dong Dazhong, Wang Shejiao, Li Jiangzhong, Li Xinjing, Wang Yuman, Li Denghua and Cheng Keming, 2010. Geological characteristics and resource potential of shale gas in China. *Petroleum Exploration & Development*, 2010, 37(6):641–653.

Zou Caineng, Yang Zhi, He Dongbo, Yu Yunsheng, Li Jian, Jia Ailin, Chen Jianjun, Zhao Qun, Li Yilong, Li Jun and Yang Shen,2018. Theory, technology and prospects of conventional and unconventional natural gas. *Petroleum Exploration & Development*, 45(04):575–587.

Zou Caineng, Yang Zhi, Pan Songqi, Chen Yanyan, Lin Senhu, Huang Jinliang, Wu Songtao, Dong Dazhong, Wang Shufang, Liang Feng, Sun Shasha, Huang Yong and Weng Dingwei, 2016. Shale Gas Formation and Occurrence in China:An Overview of the Current Status and Future Potential. *Acta Geologica Sinica* (English Edition),2016,90(04):1249–1283.

About the first author

TIAN Hua, male, born in 1986 in Baoding Jiang City, Hebei; Master, graduated from graduate school of Research Institute of Petroleum Exploration and Development, PetroChina. He is mainly engaged in research of unconventional petroleum geology. Email:tianhua86@petrochina.com.cn; phone: 010-8359 8620, 15210030853.